AGU PUBLICATIONS

Geophysical Research Letters

RESEARCH LETTER
10.1002/2016GL067728

Key Points:
- Hurricane activity after Eastern Pacific El Niño related to subsurface heat meridional movement
- Hurricane activity after Central Pacific El Niño related to vertical wind shear anomalies
- Hurricane activity following Central Pacific events is not different from neutral ENSO conditions

Supporting Information:
- Figures S1–S11 and Tables S1–S5

Correspondence to:
J. Boucharel,
j.boucharel@unsw.edu.au

Citation:
Boucharel, J., F.-F. Jin, I. I. Lin, H.-C. Huang, and M. H. England (2016), Different controls of tropical cyclone activity in the Eastern Pacific for two types of El Niño, *Geophys. Res. Lett.*, *43*, 1679–1686, doi:10.1002/2016GL067728.

Received 11 JAN 2016
Accepted 26 JAN 2016
Accepted article online 28 JAN 2016
Published online 19 FEB 2016

Different controls of tropical cyclone activity in the Eastern Pacific for two types of El Niño

Julien Boucharel[1], Fei-Fei Jin[2,3], I. I. Lin[4], Hsiao-Ching Huang[4], and Matthew H. England[1]

[1]ARC Centre of Excellence for Climate System Science, University of New South Wales, Kensington, New South Wales, Australia, [2]Department of Atmospheric Sciences, SOEST, University of Hawaii at Manoa, Honolulu, Hawaii, USA, [3]Laboratory for Climate Studies, Beijing Climate Center, Chinese Meteorological Agency, Beijing, China, [4]Department of Atmospheric Sciences, National Taiwan University, Taipei, Taiwan

Abstract The El Niño–Southern Oscillation (ENSO) is known to have different modes of expression, characterized by different dynamics and spatial anomalies patterns: the Eastern Pacific (EP) and Central Pacific (CP) El Niño. The main region of influence of the former is located in the Eastern Pacific, while CP events have a stronger signature of ocean/climate anomalies in the Central West Pacific. This leads to distinctive oceanic and atmospheric signatures that likely have different influences on tropical cyclone (TC) activity in the Eastern Pacific, the second most active region in the world. In this study we investigate the respective role of oceanic and atmospheric conditions on TC formation and intensification in the Eastern Pacific associated with these two flavors of ENSO. We find that the oceanic control, through meridional redistribution of subsurface heat, is the main driver of TC activity during the hurricane season following EP events. In contrast, atmospheric conditions tend to be destructive to TC intensification after those events. The altered atmospheric circulation, in particular the reduction of vertical wind shear and the increase in relative humidity, tends to be more influential in controlling TC activity post CP events. However, unlike for subsurface heat, these changes in atmospheric conditions are not statistically distinct between these two ENSO flavors—although they are consistent across all atmospheric data sets tested. Overall, unlike after EP El Niño events, the hurricane season activity following a CP event is not significantly different from neutral or even La Niña years.

1. Introduction

Compared to the Atlantic, the Eastern Equatorial Pacific (EPac) is often overlooked in terms of tropical cyclone (TC) activity, yet it is the second most active region globally [e.g., *Dong and Holland*, 1994; *Wang and Lee*, 2009; *Peduzzi et al.*, 2012]. This is likely due to the fact that TCs originate off the coast of Central America around 10°N and then mostly develop and intensify traveling westward, far from coastlines. However, some systems can make strong landfalls and impact the Pacific coast of Mexico and the Southwest of the U.S. [*Jauregui*, 2003; *Raga et al.*, 2013; *Ritchie et al.*, 2011; *Wood and Ritchie*, 2013]. In particular, lately, the Mexican and Californian coastlines have been severely hit by major hurricanes (e.g., *Manuel* (*Odile*) in September 2013 (2014)). Also, recent evidence suggests an increased TC activity around Hawaii associated with global warming [*Murakami et al.*, 2013], so there is a great interest and urgency to better understand the TC activity in this region.

The role of subsurface ocean temperatures on TC activity has recently received a lot of attention. Both observational and modeling studies suggest that oceanic properties such as thermocline depth or upper ocean stratification play a major role in TC intensification and maximum intensity [*Balaguru et al.*, 2013; *Lin et al.*, 2013; *Vincent et al.*, 2014; *Caron et al.*, 2015]. For example, rapid TC intensification has been linked to high values of upper ocean heat content contained in mesoscale features, such as warm eddies [*Shay et al.*, 2000]. They act as insulators between TCs and the deep ocean, as the presence of a thick ocean mixed layer in the eddy prevents the deeper cold water from being entrained into the upper ocean to fuel the TC [*Lin et al.*, 2005]. In a recent letter, *Jin et al.* [2014, hereafter JBL] uncovered a fundamental dynamical mechanism that participates in the interannual fuelling of TC activity in the EPac. They argue that the classic recharge-discharge (RD) theory [*Jin*, 1997] that provides the essential understanding of El Niño–Southern Oscillation (ENSO) variability is at the heart of year-to-year variations of hurricane activity in the region. This thermal control occurs via the meridional redistribution of subsurface heat following an El Niño event that can potentially provide sufficient energy for storms to turn into major hurricanes. The diagnostics presented by JBL were based on empirical orthogonal function (EOF) analyses over the recent period, therefore potentially biased by the occurrence of the two

strongest El Niños on record, 1982/1983 and 1997/1998, which belong to one particular class of ENSO, the so-called canonical or Eastern Pacific (EP) El Niño, [*Rasmusson and Carpenter*, 1982; *Harrison and Larkin*, 1998]. Yet the terminology "canonical" is misleading as during the past 15 years it has become apparent that there are other flavors of ENSO. Different onset time, propagation features, or spatial structures of anomalies exemplify this natural "ENSO diversity" [*Capotondi et al*., 2015]. One particular mode of ENSO expression is the so-called Central Pacific (CP) El Niño [*Yeh et al*., 2009] also named the Dateline El Niño [*Larkin and Harrison*, 2005], El Niño Modoki [*Ashok et al*., 2007], or Warm Pool El Niño [*Kug et al*., 2009]. The analyses of subsurface heat control on EPac hurricanes undertaken by JBL rely on a 3 years moving average of yearly TC activity, which tends to smooth out the "noise" of fast CP events [*Moon et al*., 2015; *Jin et al*., 2015] (Figure S1 in the supporting information). Here we investigate whether the oceanic mechanism obtained by JBL also plays a role during CP El Niño and in particular whether CP events also provide subsurface heat to fuel the EPac TC season.

Of course, atmospheric factors, such as the environmental relative humidity or vertical wind shear (respectively ERH and VWS hereafter), remain pivotal for individual storm tracking and can be just as relevant as the oceanic control on the activeness of a TC season. In particular, the sea surface temperature anomalies (SSTAs) induced by ENSO can modify atmospheric conditions, e.g., atmospheric stability, VWS, and ERH [*Dong and Holland*, 1994; *DeMaria*, 1996; *Collins and Mason*, 2000; *Collins*, 2007; *Camargo et al*., 2008].

The objective of this study is to refine the JBL results by breaking down the respective role of atmospheric versus oceanic controls of TC activity during the Northern Hemisphere hurricane season (i.e., May to November) following the two different types of El Niño events. Data are described in the following part and analyzed in section 3. Section 4 provides a discussion of our main results and concluding remarks.

2. Data and Methods

For oceanic conditions, we use the European Centre for Medium-Range Weather Forecasts (ECMWF) monthly ocean analysis system (ORA-S3) spanning the period 1959–2009 [*Balmaseda et al*., 2008]. ORA-S3 has been extensively used and validated within the climate community [e.g., *Zhai and Hu*, 2013; JBL; *Boucharel et al*., 2015]. To assess the most recent period, uncovered by ORA-S3 (2010 onward), we use the National Environmental Prediction Center real-time ocean reanalysis: the new Global Ocean Data Assimilation System, over the period 1980–2014 [*Saha et al*., 2006]. Both ocean products give similar results on their overlapping temporal period.

TC data (trajectories and intensity) are derived from the best track archives of the National Oceanic and Atmospheric Administration's (NOAA's) Tropical Prediction Center.

The VWS, i.e., the difference in wind between the 200 mb and 850 mb atmospheric levels [*DeMaria*, 1996] (cf. supporting information for more details on VWS calculation) and the ERH, i.e., the relative humidity averaged between the 700 mb and 850 mb atmospheric levels [*Kaplan and DeMaria*, 2003; *Wu et al*., 2012], come from a variety of monthly average of daily atmospheric reanalysis. One commonly used is released by the National Centers for Environmental Prediction (NCEP)-National Center for Atmospheric Research. NCEP product is examined here as it covers the longest temporal period, but we also present the analyses for the ECMWF atmospheric reanalysis, ERA-40 [*Uppala et al*., 2005], ERA-Interim [*Dee et al*., 2011], and the NASA reanalysis, Modern-Era Retrospective Analysis for Research and Applications (MERRA) [*Rienecker et al*., 2011] in the supporting information (Figures S5–S10 and Table S4).

As an integrated metric of TC activity, we use the accumulated cyclone energy (ACE) index, defined as the sum of the squares of the maximum wind speeds over all 6 h periods during which the maximum wind speed is over 35 kt for every storms [*Bell et al*., 2000]. We also considered the TC intensity (maximum wind speed average) that relates more to oceanic conditions than ACE, which encompasses atmospheric effects too [*Lin and Chan*, 2015]. All these variables are averaged in "TC region" (130–100°W, 7–17°N), slightly modified compared to JBL (Figure S11).

To delineate the respective role of ENSO-related oceanic and atmospheric controls onto the EPac TC activity during the two types of El Niño, we use a composite approach. We follow the *Kug et al*. [2009] classification to distinguish between CP and EP El Niños. Though each El Niño event has a unique spatial pattern, *Kug et al*. [2009] propose to classify them depending on the location of the maximum SSTA, Western Pacific (Niño 4 region, i.e., 160–210°E, 5°N–5°S) for CP events, and Eastern Pacific (Niño 3 region, i.e., 150–90°W, 5°N–5°S) for EP events. The events of 1977/1978, 1990/1991, 1994/1995, 2002/2003, 2004/2005, and 2009/2010 fall into the first category,

Table 1. Student's *t* Test Values With Both Single and Two-Tails Significance Levels for the Difference in TC Intensity (i.e., Maximum Wind Speed Average) Between Eastern Pacific (EP) and Central Pacific (CP) El Niño Events Over TC Region (130–100°W, 7–17°N) or the Entire North Eastern Pacific

Average Intensity TD-C5	Mean (Knots)	Variance	Sample Number	*T* Value	Confidence Level (One Tail)	Confidence Level (Two Tails)
TC Region (130–100°W, 7–17°N), (May–November) Average Intensity TD-C5						
EP El Niño (83, 87, 88, 92, and 98)	53.50	788.00	1317	*5.827*	*100%*	*>99.99%*
CP El Niño (91, 95, 03, 05, and 10)	48.41	682.85	1079			
Eastern Pacific (May–November) Average Intensity TD-C5						
EP El Niño (83, 87, 88, 92, and 98)	52.01	723.95	2563	6.468	100%	>99.99%
CP El Niño (91, 95, 03, 05, and 10)	46.90	641.16	1880			

while the events of 1972/1973, 1976/1977, 1982/1983, and 1997/1998 El Niño events belong to the second. The 1986/1987, 1987/1988, and 1991/1992 are trickier to identify, with a maximum SST anomaly located between 120° and 150°W. For all these events, the "Improved El Niño Modoki Index" as defined by *Li et al*. [2010] is below one standard deviation, while the classic Niño 3.4 index (190–240°E, 5°N–5°S) is above (Figure S2). This encourages us to categorize these events as EP El Niño. Both El Niño modes are locked to the EPac seasonal cycle and therefore peak during the boreal winter in the equatorial Pacific, typically in November, December January and February (NDJF) [*Stein et al*., 2014]; hence, the name is 1997/1998, for example, as this event peaks between November 1997 and February 1998. As shown by JBL, the meridional discharge of El Niño equatorial winter heat takes 6–9 months to reach region TC, thereby occurring during the following TC season. We also similarly evaluate atmospheric and oceanic conditions during the EPac hurricane season of neutral (1978/1979, 1979/1980, 1985/1986, 2000/2001, and 2011/2012) and La Niña (1988/1989, 1998/1999, 1999/2000, 2007/2008, and 2010/2011) years for robust statistical comparisons.

We decided to consider only the recent period (1979 onward), as it is more reliable in terms of oceanic conditions and TC statistics. Before the satellite era, storms not responsible for major landfalls, typically occurring far from inhabited coastlines, were commonly missed [*Landsea*, 2005]. Also, in situ measurements below the surface were sparse before the 1970s, so little subsurface data are available for assimilation in oceanic reanalysis products.

In the next section, we explore oceanic and atmospheric characteristics along with occurrences of TCs during the boreal TC season following the wintertime peak of both El Niño flavors.

3. Results

Table 1 presents the TC intensity average in TC region (and in the entire EPac) for both types of El Niño. Note that we have retained five events for both kinds, which thus provides an equal sampling for EP and CP flavors. The TC intensity increase from CP to EP events is significant at 100% using a Student's *t* test. Additional diagnostics can be found in the supporting information. For instance, Table S1 shows the simple TC account for each hurricane category that occurred during the boreal summer subsequent to these El Niño events. There is an increase (decrease) of 107% (14%) in the occurrence of major hurricanes (categories 3–5 in the Saffir-Simpson Scale, as compared to minor TC, i.e., category 2 and below) in seasons post EP (CP) events compared to seasons after neutral years. We also estimated the normalized grid-by-grid count of TC to obtain the percentage of major TC grids over all TC grids for each month and category of ENSO. This is a more precise measure of TC activity than the normal count, which also relates to TC genesis. We find an increase of major TC occurrence from CP to EP conditions and from neutral to EP conditions, with a statistical confidence using a Student's *t* test of, respectively, 94% and 92% (cf. Tables S2). Which ENSO-related environmental factors are responsible for such differences in TC activity between these two flavors? To address this question, we carry out a composite analysis and assess average oceanic and atmospheric conditions during the TC season following both ENSO types.

Figure 1 shows the hurricane season composite of monthly SST, subsurface temperature in the upper 80 m (T80), VWS, ERH anomalies, and TC trajectories following both ENSO flavors. Note that we define the heat content as the integrated potential temperature within the upper 80 m, as compared to JBL who use the upper 105 m. The results are very robust to the integration depth so long as it is below the depth of the shallow mixed layer (≈15/20 m in region TC). Indeed, mixed layer and thermocline dynamics are decoupled in this region on interannual timescales; the former is being mostly controlled by atmospheric variability associated with the Inter Tropical Convergence Zone, while the latter is driven by the El Niño recharge-discharge of

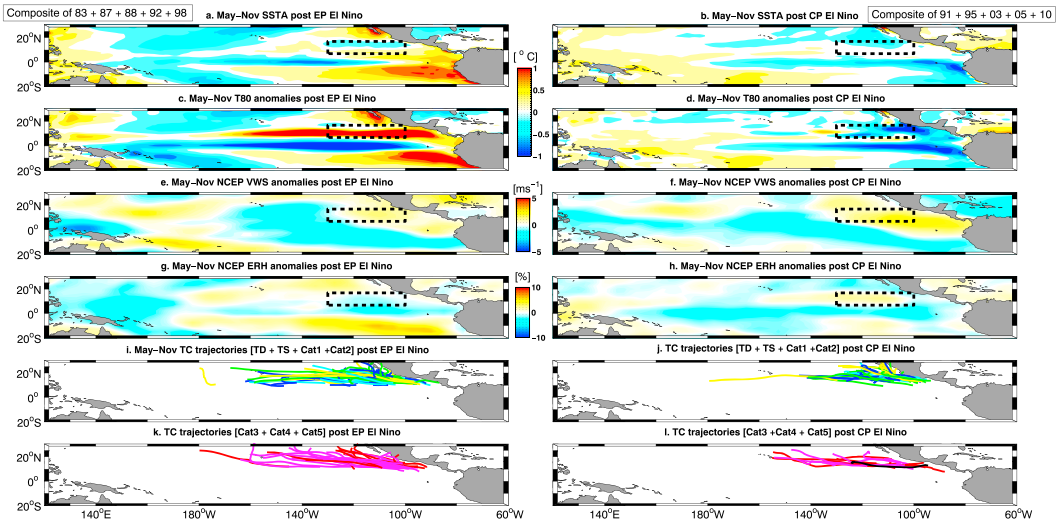

Figure 1. Composite of hurricane season averaged (May to November) monthly anomalies following (a, c, e, g, i, and k) Eastern Pacific–EP (respectively, (b, d, f, h, j, and l) Central Pacific–CP) El Niño events of SST, Figure 1a (Figure 1b); subsurface temperature averaged in the first 80 m, Figure 1c (Figure 1d); vertical wind shear, Figure 1e (Figure 1f); and environmental relative humidity from NCEP product, Figure 1g (Figure 1h). Figure 1i (Figure 1j) shows the minor tropical cyclones trajectories (tropical depressions to category 2 hurricanes) that occurred during hurricane seasons following EP (respectively, CP) El Niño events. Figures 1k and 1l show the same for major tropical cyclones (category 3 and above). The individual events used to compose EP (CP) conditions are indicated above the left (right) panels. Tropical depressions are in dark blue, tropical storms in cyan, category 1 in green, category 2 in yellow, category 3 in red, category 4 in magenta, and category 5 in black. See Table S5 for TC classification. Region TC (130–100°W, 7–17°N) is represented by the thick dashed black box in Figures 1a–1h.

subsurface heat (JBL, Figure S23). As indicated by Table S1, there is a much higher density of TC tracks for both minor and major hurricanes occurring during TC seasons post EP events (see Figures 1i and 1k compared to Figures 1j and 1l). Interestingly, there is also a noticeable difference in the location and extent of these trajectories. Hurricanes following EP El Niño are more likely to travel farther west and north toward the Hawaiian Islands, while TCs post CP events tend to stay near the American coast. *Chu and Wang* [1997] found indeed an increased TC activity during El Niño years in the vicinity of Hawaii. Their study was published before the identification of the new CP flavor, hence was based on the data from EP El Niño only available at the time. The most striking difference between anomalous conditions following CP and EP events is found in the subsurface and atmospheric variables. The SSTA is not fundamentally different at least in the region of TC formation/development (see Figures 1a and 1b). T80 summer anomalies post EP events (Figure 1c) resemble the pattern of the second EOF mode of heat content in the tropical Pacific (JBL, Figure 1b). There is a clear signature of the meridional redistribution of heat associated with the ENSO recharge-discharge mechanism [*Jin*, 1997]. Although this theory is also at play to some extent for the CP flavor of ENSO, the discharge process of equatorial heat associated with these events is weak, mostly directed south of the equator and located more in the central to Western Pacific [*Ren and Jin*, 2013], far from the EPac TC formation region (cf. Figure 1d). Therefore, this off-equatorial CP ENSO heat will not be available to influence TC intensification in the EPac. In addition, T80 anomalies are strongly negative after CP events in TC region, therefore unfavorable for storm intensification during the hurricane season after this type of event.

VWS anomalies exhibit fairly similar patterns for these two flavors of ENSO (Figures 1e and 1f) but have contrasting sign for both ECMWF products (Figures S5 and S7). This highlights the uncertainty associated with atmospheric reanalysis fields. Except along a band east of Hawaii, VWS anomalies appear to be mostly positive in the tropical Pacific post EP El Niño, therefore detrimental to TC formation and strengthening. Similarly, ERH anomalies display opposite distribution between these two types of El Niño (Figures 1g and 1h) and support previous conclusions. Negative ERH anomalies in the main region of TC intensification (TC region, delineated by the dashed black box in Figure 1) are unfavorable to TC intensification after EP events. Again, as evidenced by JBL, this emphasizes the stronger control of El Niño-induced ocean heat content than El Niño-induced atmospheric perturbations on TC activity for the EP mode (i.e., the disruption of atmospheric fields such as VWS and ERH by ENSO-driven SST anomalies). However, the presence of weaker than usual

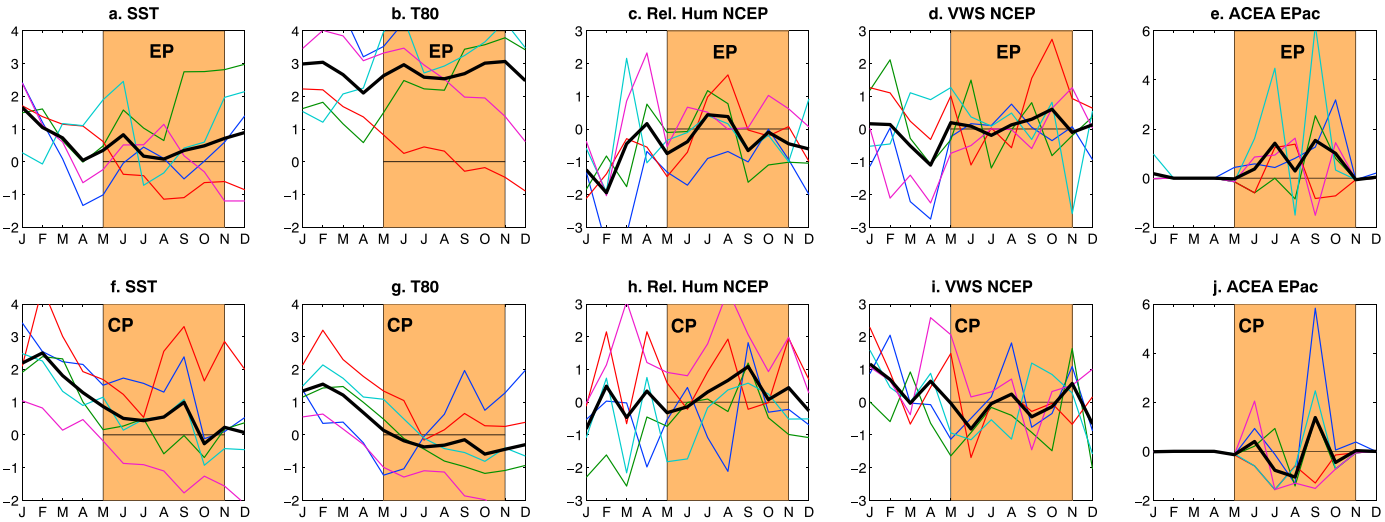

Figure 2. Evolution (a and f) of SST anomalies, (b and g) subsurface temperature anomalies averaged in the first 80 m, (c and h) environmental relative humidity anomalies, (d and i) vertical wind shear anomalies from NCEP product, and (e and j) ACE anomalies leading up to and during the Eastern Pacific hurricane season (May until November (MJJASON), shaded in orange) following Eastern Pacific (EP) El Niño events (Figures 2a–2e) and following Central Pacific (CP) El Niño events (Figures 2f–2j). Anomalies are averaged in TC region (130–100°W, 7–17°N, region delineated in Figure 1). Thin colored lines represent variables for different El Niño episodes used to average the "composite" variable (thick black line). Note that all time series have been normalized by their standard deviation.

VWS east of Hawaii provides favorable conditions for TCs to potentially continue their trajectory toward the Central Pacific, a region where T80 anomalies return to neutral, away from the discharged heat of EP El Niño [*Chu and Wang*, 1997]. The VWS (ERH) in ECMWF products anomaly patterns in hurricane seasons post CP events is of the opposite sign for seasons post EP events, with negative (positive) anomalies in the TC region, both favorable to TC formation. The increased VWS anomalies in the northeast Pacific post CP events are detrimental to TC intensification and north-westward moving tracks. This is clear in ERA reanalysis (Figures S5 and S7) but not as obvious in NCEP product (Figure 1). Despite these uncertainties, the difference in VWS and ERH anomalies might explain the large difference in the number of major hurricanes (see Table 1) between the two ENSO modes, as well as the greater extent of TC tracks toward the central north Pacific during hurricane seasons post EP El Niño events (Figures 1, S5, and S7i–S7l).

Figure 2 shows the temporal evolution of atmospheric and oceanic conditions as well as TC activity averaged in TC region from the wintertime peak of El Niño in January until the end of the calendar year for both types of ENSO. Oceanic variables display very different behaviors between the different varieties of El Niño. Coinciding to the spatial pattern of the second mode of SSTA EOF characteristic of CP El Niño, which extends from the central equatorial Pacific to the north EPac [*Ashok et al.*, 2007], we observe a boreal winter peak of SSTA followed by a decline toward cooler SST than usual during summer/fall in TC region (Figure 2f). The heat content exhibits similar behavior with cold anomalies also occurring during the second half of the year (Figure 2g), clearly indicative of unfavorable oceanic conditions for TC intensification post CP events. In contrast, after EP El Niño, both warm surface and subsurface anomalies exhibit a reversed evolution from weak anomalies in boreal winter to anomalously warm conditions during the subsequent summer/fall in the EPac. This illustrates the discharge of warm equatorial wintertime anomalies toward TC region throughout the second half of the year [*Jin*, 1997; JBL]. Interestingly, subsurface anomalies display two maxima, one in June–July and the other in September–October (Figure 2b), which are concurrent with peaks in ACE anomalies (Figure 2e). This validates the JBL conclusion for the EP El Niño type, namely, that the warm equatorial subsurface anomalies discharged into the EPac can promote TC intensification leading to an abnormally active hurricane season. The evolution of VWS and ERH anomalies post EP events confirms the dominant oceanic control on TC activity for this variety of ENSO (Figures 2c and 2d). Indeed, the VWS (ERH) tends to be enhanced (decreased), therefore more destructive to TC intensification in the EPac during hurricane seasons following EP El Niño. In contrast, after a CP event, VWS (ERH) is weaker (stronger) than usual in May–June and September–November but enhanced (diminished) in July–September (Figures 2h and 2i). The ACE anomalies follow a reversed evolution with a suppressed TC activity during July–September but a stronger intensity early and late in the season

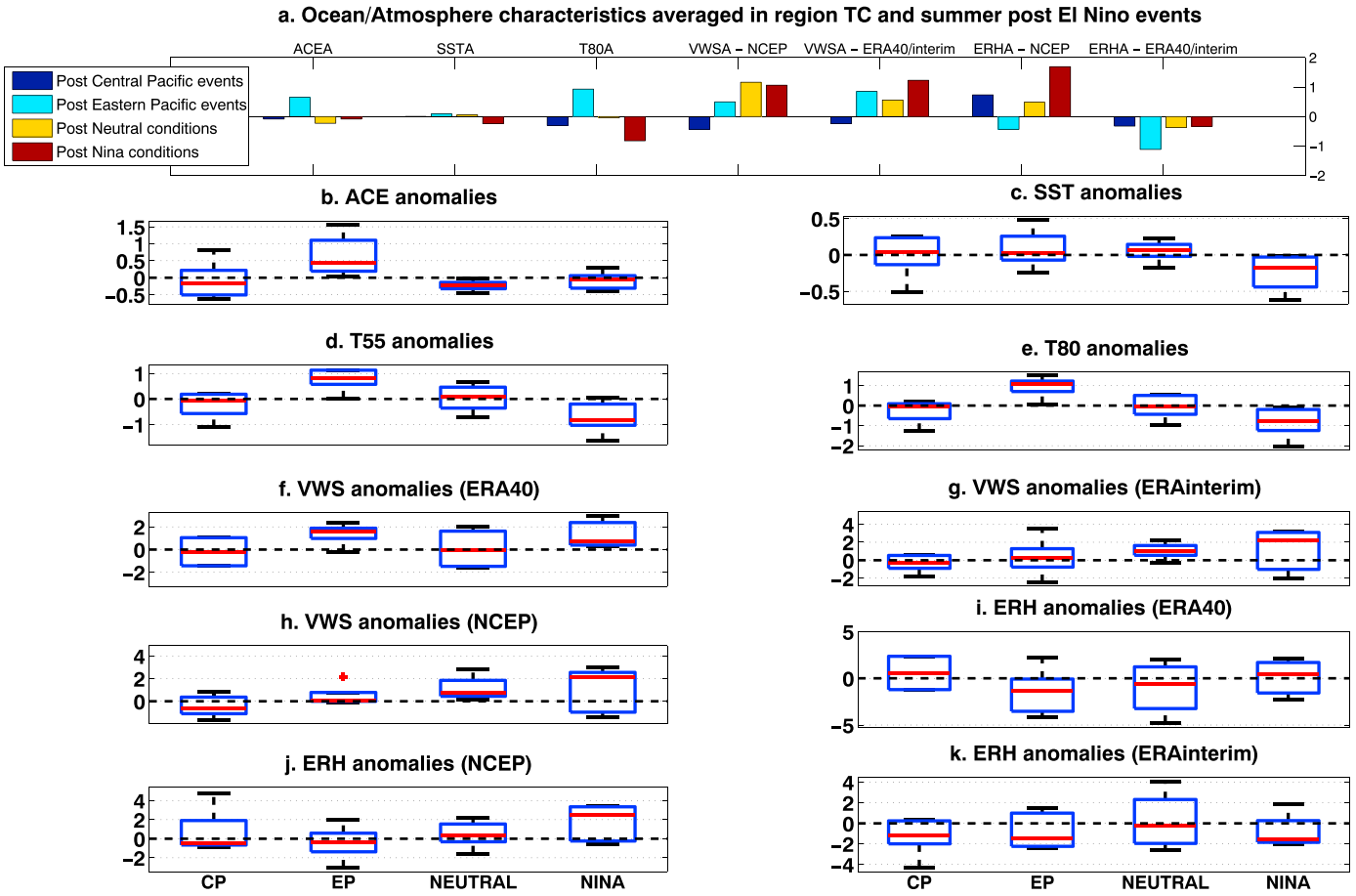

Figure 3. Hurricane season (May–November) average of different oceanic and atmospheric variables and ACE for composite post CP (blue), EP (cyan) El Niño, neutral (yellow), and La Niña (red) (see Table S1 for details) conditions and for different atmospheric reanalysis products. It represents the average of Figures 2 and S4 thick black lines over the orange shaded time period. Figures 3b–3i represent the distributions of the oceanic and atmospheric variables and ACE. The boxes show the 25th–75th percentile range; the whiskers, the interevents range, and the median are marked in red.

(Figure 2j). Although not statistically different from the EP type (cf. supporting information), altered atmospheric conditions follow the same evolution in all reanalysis products tested during CP El Niño years and seem to exert a stronger control than oceanic characteristics on TC activity in the EPac. The distinct oceanic and atmospheric teleconnections of these two flavors of ENSO thus lead to significantly different TC activities.

Figure 3 provides a statistical summary of several oceanic and atmospheric variables averaged over the hurricane season (orange shaded area in Figure 2) for the two types of El Niño as well as for neutral and La Niña years for reference (Figures S3, 4, and Table S1). TC activity is significantly enhanced after EP events as compared to post CP and neutral and La Niña conditions (Figure 3b). SSTAs are relatively similar in TC region regardless of the ENSO conditions (Figure 3c). In contrast, we observe statistically significant changes between the two flavors of ENSO in the EPac oceanic subsurface (Figures 3d and 3e) and atmospheric conditions to some extent (Figures 3f–3k). In particular, despite statistical uncertainties associated with atmospheric variables, in all atmospheric reanalysis data VWS is consistently slightly positive (negative) after EP (CP) events, therefore detrimental (favorable) to TC intensification. ERH is negative (positive) during the hurricane season post EP (CP) events and, thus similar to VWS, is clearly unfavorable (favorable) to TC intensification. Atmospheric conditions post EP events are not statistically distinguishable from neutral or even Niña conditions and therefore have little influence on TC activity in the EPac (Figures 3f–3k). On the other hand, ocean heat content is much higher in TC region after an EP event and is the clear driver of hurricane activity in this region, whereas subsurface heat post CP events are not significantly different from neutral or cold ENSO conditions (Figures 3d and 3e). This underscores the different controls and in particular the stronger influence of ocean heat content on hurricane activity in the EPac between these two types of El Niño.

4. Conclusions

The analyses presented here reveal distinct signatures of TC activity in the EPac associated with the two different modes of ENSO expression, as a follow up to the recent study of JBL. They found that the ENSO RD mechanism facilitates the main supplier of heat for tropical storms to grow into major hurricanes, through the off-equatorial discharge of subsurface heat into the TC formation region. However, this mechanism only operates after EP El Niño and is not sufficient to fuel hurricane activity after CP El Niño. In fact, in contrast to EP events, and despite statistical uncertainties, the altered atmospheric circulation (consistent across all reanalysis products analyzed here) seems more influential in controlling TC activity during hurricane seasons following CP events. In particular, the extension of SSTA towards the cyclogenesis region for this ENSO flavor can induce weaker VWS and stronger ERH anomalies in the EPac, which in turn can promote favorable conditions for TC formation and intensification. Finally, regardless of these different controls, the occurrence of strong EP El Niño leads to significantly more active hurricane seasons compared to the TC activity following CP events, which are not significantly different from normal year or even La Niña conditions.

Acknowledgments

This project was supported by the Australian Research Council (FL100100214); US National Science Foundation grants ATM1034798, ATM1049219, and ATM1406601; US Department of Energy grant DESC005110; US NOAA grant NA10OAR4310200; the China Meteorological Special Project (GYHY201206033); and the 973 Program of China (2010CB950404 and 2013CB430203). I.I.L.'s work is supported by Taiwan's Ministry of Science and Technology under grants NSC 101-2111-M-002-002-MY2, NSC 101-2628-M-002-001-MY4, and 102R7803. I.I.L. wants to acknowledge Chun-Chi Lien for help in data analysis. We thank two anonymous reviewers for their constructive comments. TC data can be found at NOAA's Tropical Prediction Center, http://www.nhc.noaa.gov/?epac, ORA-S3 data at http://apdrc.soest.hawaii.edu/datadoc/ecmwf_oras3.php, NCEP data at http://www.esrl.noaa.gov/psd/data/gridded/data.ncep.reanalysis.derived.surface.html, and ERA data at http://apps.ecmwf.int/datasets/. We want to acknowledge the Global Modeling and Assimilation Office (GMAO) and the GES DISC for the dissemination of MERRA (http://disc.sci.gsfc.nasa.gov/daac-bin/DataHoldings.pl).

References

Ashok, K., S. K. Behera, S. A. Rao, H. Weng, and T. Yamagata (2007), El Niño Modoki and its possible teleconnection, *J. Geophys. Res.*, *112*, C11007, doi:10.1029/2006JC003798.

Balaguru, K., R. L. Leung, and J.-H. Yoon (2013), Oceanic control of northeast Pacific hurricane activity at interannual timescales, *Environ. Res. Lett.*, *8*, 044009.

Balmaseda, M. A., A. Vidard, and D. L. T. Anderson (2008), The ECMWF ocean analysis system: ORA-S3, *Mon. Weather Rev.*, *136*, 3018–3034.

Bell, G. D., M. S. Halpert, R. C. Schnell, R. W. Higgins, J. Lawrimore, V. E. Kousky, R. Tinker, W. Thiaw, M. Chelliah, and A. Artusa (2000), Climate assessment for 1999, *Bull. Am. Meteorol. Soc.*, *81*, S1–S50.

Boucharel, J., A. Timmermann, A. Santoso, M. H. England, F.-F. Jin, and M. A. Balmaseda (2015), A surface layer variance heat budget for ENSO, *Geophys. Res. Lett.*, *42*, 3529–3537, doi:10.1002/2015GL063843.

Camargo, S. J., A. H. Sobel, A. G. Barnston, and M. Ghil (2008), Clustering of eastern north Pacific tropical cyclone tracks: ENSO and MJO effects, *Geochem. Geophys. Geosyst.*, *9*, Q06V05, doi:10.1002/2015GL063843.

Capotondi, A., et al. (2015), Understanding ENSO diversity, *Bull. Am. Meteorol. Soc.*, *96*, 921–938.

Caron, L.-P., M. Boudreault, and S. J. Camargo (2015), On the variability and predictability of eastern north Pacific tropical cyclone activity, *J. Clim.*, doi:10.1175/JCLI-D-15-0377.1.

Chu, P. S., and J. Wang (1997), Tropical cyclone occurrences in the vicinity of Hawaii: Are the differences between El Niño and non-El Niño years significant?, *J. Clim.*, *10*, 2683–2689.

Collins, J. M. (2007), The relationship of ENSO and relative humidity to interannual variations of hurricane frequency in the northeast Pacific Ocean, *Pap. Appl. Geogr. Conf.*, *30*, 324–333.

Collins, J. M., and I. M. Mason (2000), Local environmental conditions related to seasonal tropical cyclone activity in the northeast Pacific basin, *Geophys. Res. Lett.*, *27*, 3881–3884, doi:10.1029/2000GL011614.

Dee, D. P., et al. (2011), The ERA-Interim reanalysis: Configuration and performance of the data assimilation system, *Q. J. R. Meteorol. Soc.*, *137*, 553–597, doi:10.1002/qj.828.

DeMaria, M. (1996), The effect of vertical shear on tropical cyclone intensity change, *J. Atmos. Sci.*, *53*, 2076–2087.

Dong, K., and G. J. Holland (1994), A global view of the relationships between ENSO and tropical cyclone frequencies, *Acta Meteorol. Sin.*, *8*, 19–29.

Harrison, D. E., and N. K. Larkin (1998), El Niño-Southern Oscillation sea surface temperature and wind anomalies, 1946–1993, *Rev. Geophys.*, *36*, 353–399, doi:10.1029/98RG00715.

Jauregui, E. (2003), Climatology of landfalling hurricanes and tropical storms in Mexico, *Atmosfera*, *16*(4), 193–204.

Jin, F. F. (1997), An equatorial ocean recharge paradigm for ENSO. Part I: Conceptual model, *J. Atmos. Sci.*, *54*, 811–829.

Jin, F.-F., J. Boucharel, and I. I. Lin (2014), Eastern Pacific tropical cyclones intensified by El Niño delivery of subsurface ocean heat, *Nature*, *516*, 82–85.

Jin, F.-F., J. Boucharel, and I. I. Lin (2015), Reply to Moon, I. J., Kim, S. H. & Wang, C., *Nature*, *526*, E5–E6, doi:10.1038/nature15547.

Kaplan, J., and M. DeMaria (2003), Large-scale characteristics of rapidly intensifying tropical cyclones in the North Atlantic basin, *Weather Forecast.*, *18*(6), 1093–1108, doi:10.1175/1520-0434(2003)018<1093:LCORIT>2.0.CO;2.

Kug, J.-S., F.-F. Jin, and S.-I. An (2009), Two types of El Niño events: Cold tongue El Niño and warm pool El Niño, *J. Clim.*, *22*, 1499–1515.

Landsea, C. W. (2005), Meteorology, hurricanes and global warming, *Nature*, *438*, E11–E12, doi:10.1038/nature04477.

Larkin, N. K., and D. E. Harrison (2005), On the definition of El Niño and associated seasonal average U.S. weather anomalies, *Geophys. Res. Lett.*, *32*, L13705, doi:10.1029/2005GL022738.

Li, G., B. Ren, C. Yang, and J. Zheng (2010), Indices of El Niño and El Niño Modoki: An improved El Niño Modoki Index, *Adv. Atmos. Sci.*, *27*, 1210–1220.

Lin, I. I., and J. C. L. Chan (2015), Recent decrease in typhoon destructive potential and global warming implications, *Nat. Commun.*, *6*, 7182, doi:10.1038/ncomms8182.

Lin, I. I., C. C. Wu, K. A. Emanuel, I. H. Lee, C. R. Wu, and I. F. Pun (2005), The interaction of Supertyphoon Maemi (2003) with a warm ocean eddy, *Mon. Weather Rev.*, *133*, 2635–2649.

Lin, I. I., P. Black, J. F. Price, C.-Y. Yang, S. S. Chen, C.-C. Lien, P. Harr, N.-H. Chi, C.-C. Wu, and E. A. D'Asaro (2013), An ocean coupling potential intensity index for tropical cyclones, *Geophys. Res. Lett.*, *40*, 1878–1882, doi:10.1002/grl.50091.

Moon, I. J., S. H. Kim, and C. Wang (2015), El Niño and intense tropical cyclones, *Nature*, *526*, E4–E5, doi:10.1038/nature15546.

Murakami, H., B. Wang, T. Li, and A. Kitoh (2013), Projected increase in tropical cyclones near Hawaii, *Nat. Clim. Change*, *3*, 749–754.

Peduzzi, P. B., et al. (2012), Global trends in tropical cyclone risk, *Nat. Clim. Change*, *2*, 289–294.

Raga, G. B., B. Bracamontes-Ceballos, L. M. Farfán, and R. Romero-Centeno (2013), Landfalling tropical cyclones on the Pacific coast of Mexico: 1850–2010, *Atmósfera*, *26*(2), 209–220.

Rasmusson, E. M., and T. H. Carpenter (1982), Variations in tropical sea surface temperature and surface wind fields associated with the Southern Oscillation/El Niño, *Mon. Weather Rev.*, *110*, 354–384.
Ren, H. L., and F.-F. Jin (2013), Recharge oscillator mechanisms in two types of ENSO, *J. Clim.*, *26*, 6506–6523.
Rienecker, M. M., et al. (2011), MERRA: NASA's Modern-Era Retrospective Analysis for Research and Applications, *J. Clim.*, *24*, 3624–3648, doi:10.1175/JCLI-D-11-00015.1.
Ritchie, E. A., K. M. Wood, D. S. Gutzler, and S. R. White (2011), The influence of eastern Pacific tropical cyclone remnants on the southwestern United States, *Mon. Weather Rev.*, *139*, 192–210.
Saha, S., et al. (2006), The NCEP climate forecast system, *J. Clim.*, *19*, 3483–3517.
Shay, L. K., G. J. Goni, and P. G. Black (2000), Effects of a warm oceanic feature on Hurricane Opal, *Mon. Weather Rev.*, *128*, 1366–1383.
Stein, K., A. Timmermann, N. Schneider, F.-F. Jin, and M. F. Stuecker (2014), ENSO seasonal synchronization theory, *J. Clim.*, *27*, 5285–5310, doi:10.1175/JCLI-D-13-00525.1.
Uppala, S. M., et al. (2005), The ERA-40 re-analysis, *Q. J. R. Meteorol. Soc.*, *131*, 2961–3012, doi:10.1256/qj.04.176.
Vincent, E. M., K. A. Emanuel, M. Lengaigne, J. Vialard, and G. Madec (2014), Influence of upper-ocean stratification interannual variability on tropical cyclones, *J. Adv. Model. Earth Syst.*, *6*, 680–699, doi:10.1002/2014MS00032.
Wang, C., and S. Lee (2009), Co-variability of tropical cyclones in the North Atlantic and the eastern North Pacific, *Geophys. Res. Lett.*, *36*, L24702, doi:10.1029/2009GL041469.
Wood, K. M., and E. A. Ritchie (2013), An updated climatology of tropical cyclone impacts on the southwestern United States, *Mon. Weather Rev.*, *141*, 4322–4336.
Wu, L., H. Su, R. G. Fovell, B. Wang, J. T. Shen, B. H. Kahn, S. M. Hristova-Veleva, B. H. Lambrigtsen, E. J. Fetzer, and J. H. Jiang (2012), Relationship of environmental relative humidity with North Atlantic tropical cyclone intensity and intensification rate, *Geophys. Res. Lett.*, *39*, L20809, doi:10.1029/2012GL053546.
Yeh, S.-W., J.-S. Kug, B. Dewitte, M.-H. Kwon, B. P. Kirtman, and F.-F. Jin (2009), El Niño in a changing climate, *Nature*, *461*, 511–514.
Zhai, F., and D. Hu (2013), Revisit the interannual variability of the North Equatorial Current transport with ECMWF ORA-S3, *J. Geophys. Res. Oceans*, *118*, 1349–1366, doi:10.1002/jgrc.20093.